 doi:10.20944/preprints202207.0288.v1

Design, Construction and Characterization of Sealed Tube Medium Power CO_2 Laser System

Muddasir Naeem[1*], Tayyab Imran[1], Mukhtar Hussain[2], Arshad Saleem Bhatti[3]

[1]*Group of Laser Development (GoLD), Department of Physics, Syed Babar Ali School of Science and Engineering, Lahore University of Management Sciences (LUMS), Lahore 54792, Pakistan. muddasirnaeem98@gmail.com (M.N.); tayyab_imran@lums.edu.pk (T.I.)*

[2]*Department of Physics, University of Central Florida, Orlando, FL 32816, USA. mukhtar.hussain@ucf.edu (M.H.)*

[3]*M.A. Jinnah Campus, Virtual University, Defence Road, Off Raiwind Road, Lahore 54660, Pakistan. asbhatti@comsats.edu.pk (A.S.B.)*

**Corresponding email: muddasirnaeem98@gmail.com*

Abstract **–** A low-cost medium power carbon dioxide (CO_2) laser system is designed, constructed, and characterized to produce coherent, monochromatic laser radiation in the Infrared region. The laser cavity is simulated and designed by using ZEMAX optic studio. A switch-mode high tension pump source is designed and constructed using a flyback transformer and simulated using NI Multisim to study the voltage behavior at different node points. A prototype cooling system/chiller is designed and built using the Thermo-Electric Coolers (TEC) to remove the excess heat produced during laser action. Various parameters, like pumping mechanism, chiller stability, efficiency, output power, and current at different applied voltages, are studied. The chiller efficiency at different output powers of the laser is analyzed, which clearly shows that the chiller's cooling rate is good enough to compensate for the heat generated by the laser system. The center wavelength of the carbon dioxide laser is 10.6μm with FWHM of 1.2nm simulated in the ZEMAX optic studio. The output beam penetration through salt rock (NaCl), wood, and acrylic sheet at various output powers is analyzed to measure the penetration depth rate of the CO_2 laser.

Keywords **–** ***ZEMAX, Thermoelectric coolers, Flyback transformer, High tension pump source, Penetration depth.***

1. INTRODUCTION

Kumar Patel [1] reported a CW output of about 1mW using molecular vibrational-rotational transitions of carbon dioxide (CO_2) electronic ground state [2]. In 1969, Philip L. Hanst and John A. Morreal designed and tested a CO_2 laser system with two gas absorption cells built into the cavity. High-powered pulsed operation at varying wavelengths ranging from 9.08 microns to 10.6 microns at repeat frequencies of up to 100 kHz has been accomplished by the correct range of absorbing gases [3]. A low-pressure continuous-wave CO_2 laser for single line application is planned and built in 1981. This laser works in a single axial mode with a frequency stabilization of greater than 100 kHz at the peak of the power profile. The peak power varies from 0.1 to 5 Watts [4]. In 1997, a high-power 24-channel radial array slab RF excited carbon dioxide laser referred to as the Zodiac geometry was built [5]. A transverse flow transversely excited (TFTE) CW CO_2 with a maximum output power of about 15 kW has been developed by A.K. Nath, T. Reghu. The laser was operated up to 15 kW output power in four different modes viz. continuous wave mode, periodic

Preprints (www.preprints.org) | NOT PEER-REVIEWED | Posted: 19 July 2022 doi:10.20944/preprints202207.0288.v1

pulse mode, single-shot mode, and processing velocity-dependent power mode with 1.2 kHz modulation bandwidth [6]. Our approach is straightforward in making the CO_2 laser. We used a sealed tube CO_2 laser and developed the high-tension pump source and non-conventional cooling system for the tube.

This paper is about designing, constructing, and characterizing a low-cost medium power CO_2 laser system with a switch-mode power supply and prototype type cost-effective homemade chiller. A cost-effective prototype chiller is designed and fabricated using Thermoelectric coolers and small aluminum blocks.

2. DESIGN AND SIMULATION OF CO_2 LASER CAVITY

The laser cavity design is carried out using Zemax Optic Studio [7] software. When all the surfaces are defined for all relevant parameters involved in the design, the ZEMAX provides a 2D layout and shaded design model [8,9]. A reflecting mirror, focusing lens, and detector are used to detect the beam and analyze it in the design. The incident flux on the surface is referred to as irradiance and is measured as power per unit area. When the applied voltage across the laser cavity increases, more photons are delivered inside the cavity and output power increases linearly.

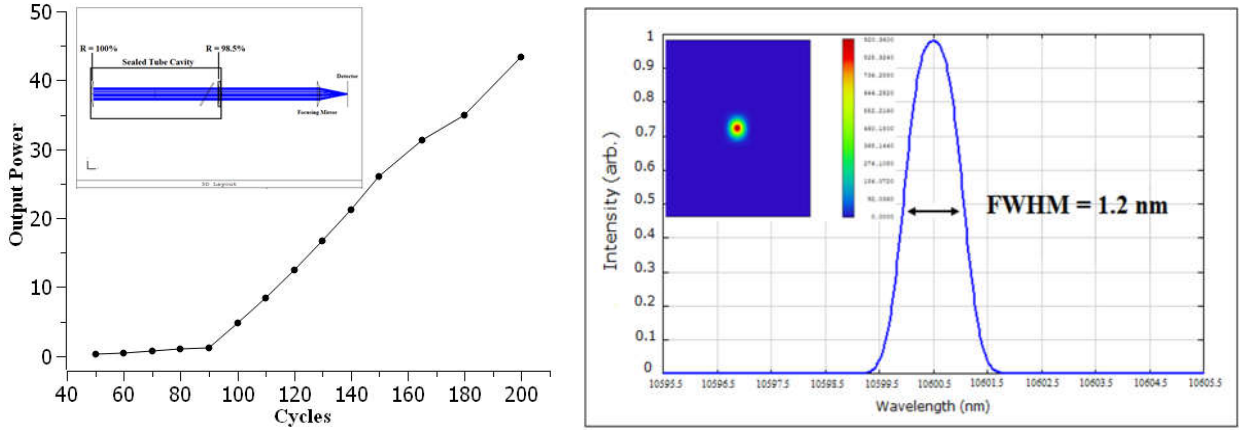

(a) **(b)**

Fig. 1: (a) Output power variation w.r.t number of cycles in the cavity (inset: 2D layout of the cavity) **(b)** Output beam spectrum of design laser cavity in Zemax Optic Studio (inset: beam spot)

Fig 1(a) shows the output power variation with the number of cycles within the cavity designed in the ZEMAX. It shows that with the increase in cycles that cause the stimulated emission in the laser cavity, the output power of the laser beam increases.

The output of the CO_2 laser system lies in the IR region. Fig 1(b) shows the output beam spectrum of the laser cavity designed in the ZEMAX optic studio. For spectrum, a diffraction grating is placed at the output of the laser cavity. The output beam is resolved into its components, and a Gaussian shape spectrum at the output is obtained.

The simulated result shows the central wavelength at 10.6 μm with FWHM of 1.2nm, as shown in Fig 1(b), which confirms the emission of the laser system in the IR region. This irradiance plot represents the top

Preprints (www.preprints.org) | NOT PEER-REVIEWED | Posted: 19 July 2022 doi:10.20944/preprints202207.0288.v1

view of the Gaussian spectrum, and irradiance changes symmetrically on both sides from the center of the beam spot.

3. DESIGN SIMULATION OF HIGH-TENSION PUMP SOURCE

The high-tension pump source circuit is designed and simulated to understand the voltage behavior and its waveform. This circuit [Fig 2(a)] is implemented in designing and fabricating the high-tension pump source. NI Multisim electrical/electronic circuit simulation software tools were used for these simulations [10,11,12].

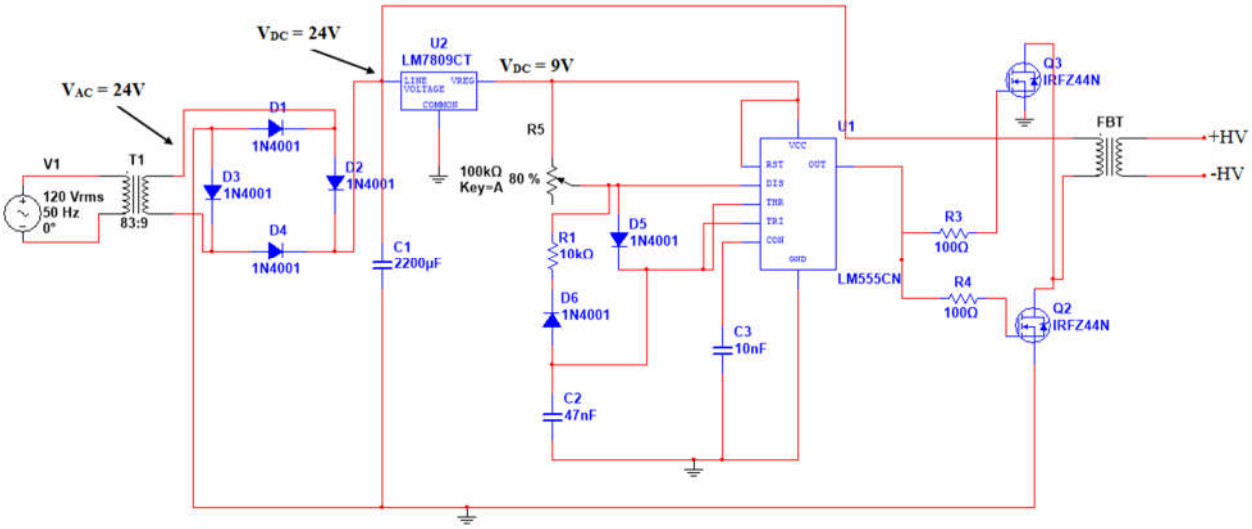

(a)

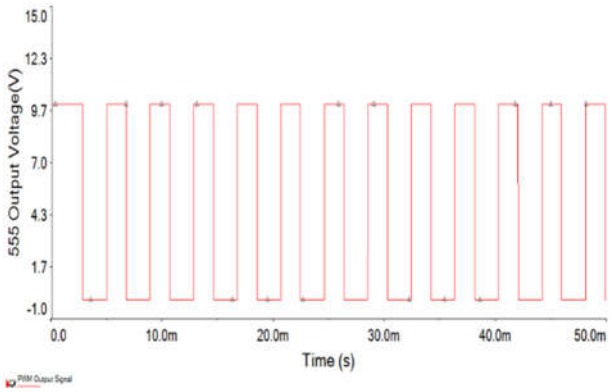

(b)

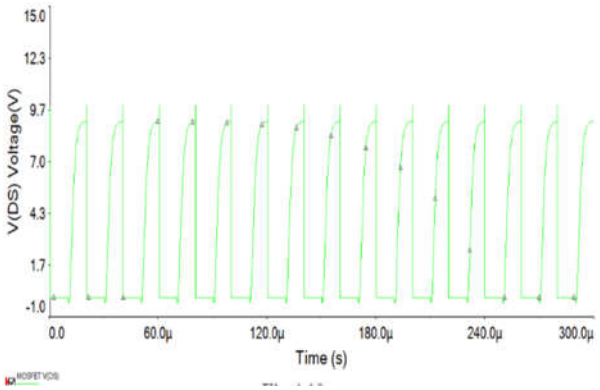

(c)

Preprints (www.preprints.org) | NOT PEER-REVIEWED | Posted: 19 July 2022 doi:10.20944/preprints202207.0288.v1

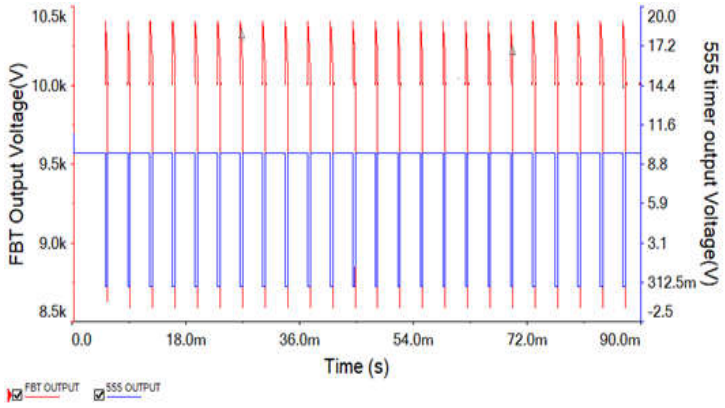

(d)

Fig. 2: (a) Circuit diagram of High-Tension Pump Source **(b)** Pulse Width Modulation (PWM) output voltage waveform **(c)** Voltage behavior across the drain to source when square wave voltage is applied at the Gate of MOSFET **(d)** Output voltage waveform of PWM and flyback transformer

The graph [Fig 2(b)] shows the simulation of a square wave generation at the output of 555-timer-based Pulse Width Modulation (PWM). The frequency of the square wave voltage can be changed by varying the capacitor or resistance values [13,14,15].

The waveform of the output pulses [Fig 2(c)] shows the behavior of the MOSFET IRFZ44 when a PMW's square wave signal is applied to the Gate. The voltage [Fig 2(a)] at the Gate controls the drain to the Source current [16]. The graph [Fig 2(d)] shows the output of 555-timer-based PWM (Blue) and Flyback transformer (Red). When the peak of the square wave signal from the PWM approaches the Gate of the MOSFET, the current starts flowing in the flyback transformer's primary coil through the drain to the source; during this time, there is no voltage at the output of the flyback transformer. When the lowest point of the square wave signal reaches the Gate of the MOSFET, no current flows through the primary of the flyback transformer. Still, the magnetic field collapses in the core, very high voltage is induced in the secondary coil of the flyback transformer, and the current starts flowing through the load. This cycle is repeated again and again to produce high voltage pulses [17,18].

4. PROTOTYPE COOLING SYSTEM FOR LASER TUBE

A large amount of heat is produced during the laser operation, affecting the laser's stability. A prototype cooling system is designed to remove this excess heat. In the laser tube's cavity, the heat produced at different rates depends on the laser system's output power. As the output power increases, the heat generated in the laser tube's cavity also increases. An efficient cooling system is designed and constructed using thermoelectric coolers. The chiller's cooling rate is 0.7^0C/min, which is enough to compensate for the heat generated by the cavity and make it stable for an extended period of its operation. The cooling system is shown in Fig 3(a).

Preprints (www.preprints.org) | NOT PEER-REVIEWED | Posted: 19 July 2022 doi:10.20944/preprints202207.0288.v1

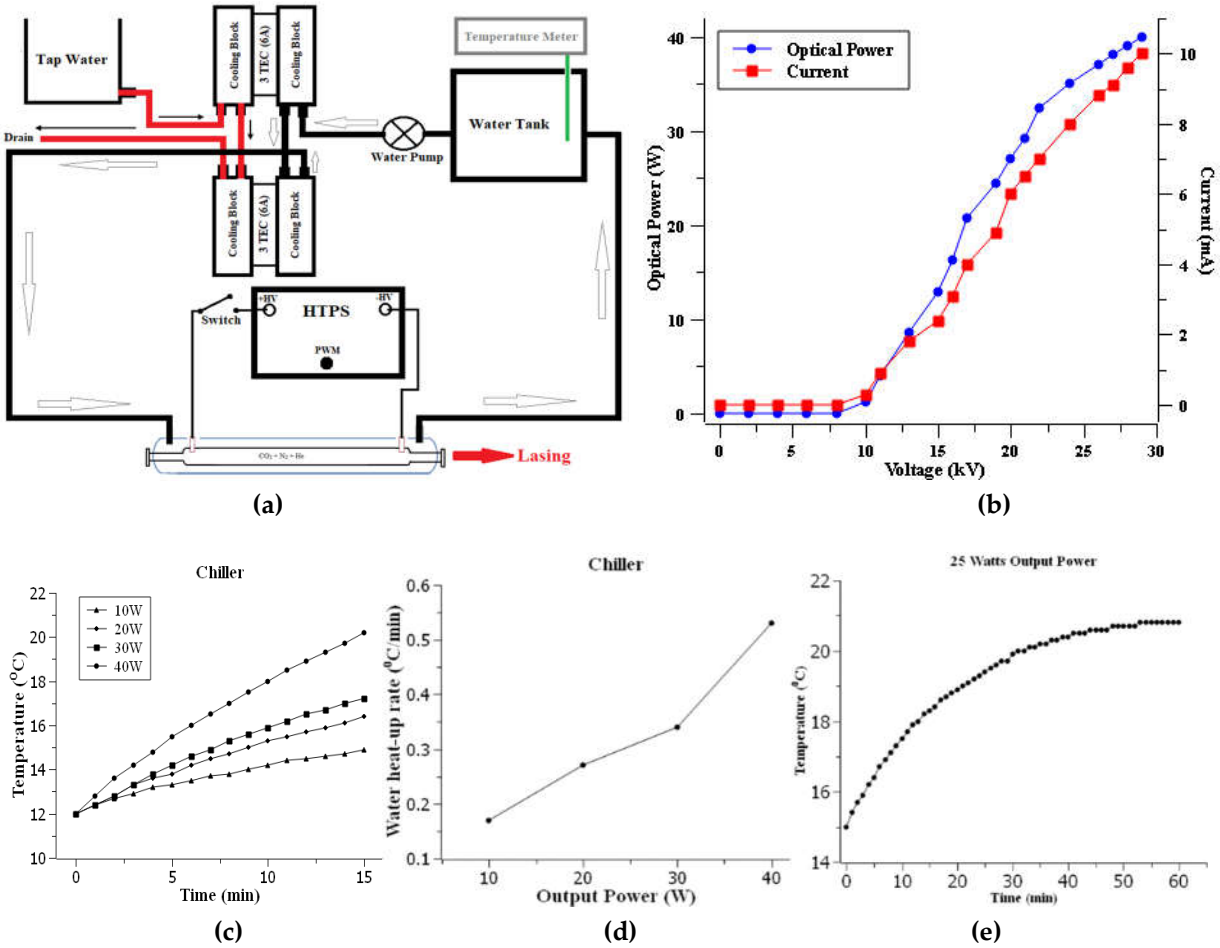

Fig. 3: (a) Complete laser system with cooling system and high-tension pump source connections **(b)** Variation of laser output power and current along applied voltage **(c)** Variation in water temperature at different output powers **(d)** Output power vs. water heat-up rate **(e)** Chiller behavior at a moderate output power for an extended period of operation

In total, six thermoelectric coolers and four aluminum blocks are used to design the cooling system. A set of three thermoelectric coolers (TEC) are a sandwich between the two aluminum blocks. In the cooling system, the water circulates in two loops. The de-ionized water is stored in the water tank. A water pump is attached to the water tank. The water is pumped from the water tank and circulates in the aluminum block connected to the cold side of the thermoelectric coolers. The heat is extracted from the water when it circulates in the aluminum blocks. The extracted heat is transferred to the hot side of the thermoelectric coolers. The de-ionized water is made to pass through another aluminum block connected to the cold side of the thermoelectric coolers. The cold water through pipes circulates in the laser tube, extracts heat from the laser cavity, and goes back to the water tank. Another aluminum block is attached to remove the heat from the hot side of the thermoelectric coolers. Tap water circulates in the aluminum block attached to the hot side of the thermoelectric coolers, extracts the heat from the hot side, and enhances efficiency. This cycle repeats continuously, and the cooling system efficiently removes the heat produced in the laser cavity during laser action.

Preprints (www.preprints.org) | NOT PEER-REVIEWED | Posted: 19 July 2022 doi:10.20944/preprints202207.0288.v1

The graph [Fig 3(c)] compares the water temperature variation at different output powers. Initially, the water temperature was 10^0C. As the laser output power increases, more heat is produced, and water temperature increases slowly. The cavity is stable because the water temperature is maintained at a certain level at which it can compensate for the heat produced by the laser action. The graph [Fig 3(d)] shows that the water heating rate increases with the laser's output power. The water heating rate is less than the cooling rate. The laser can be operated for an extended period without any problem. In graph [Fig 3(e)] the cooling efficiency during the extended period of laser operation is shown. The graph shows that the water temperature increased with time and became stable at one point, after which the cooling rate of the chiller became equal to the heating rate of water. The output power of the laser system remains stable during that period.

5. CHARACTERIZATION OF THE LASER SYSTEM

The block diagram [Fig 3(a)] shows the chiller, laser tube, and high-tension pump source connections. A sealed laser tube is used, which is filled with Carbon dioxide (CO_2), Nitrogen (N_2), and Helium (He). The ratio of the CO_2, N_2, and He is 1:2:7, respectively. The high-tension pump source is connected to the electrodes of the laser tube. The cooling system is associated with the tube through pipes, black to extract the heat from the cavity and red to extract the heat from the hot side of the thermoelectric cooler to improve the efficiency. Specification of sealed laser tube is given in Table 1.

Table 1. Specifications of sealed laser tube

Power	**40 W**
Length	70 cm
Outer Cylinder Diameter	5 cm
Inner Cylinder Diameter	2 cm
Triggering Voltage	9 kV
Working Voltage	10 kV
Power Stability	± 5%
Triggering Current	5 mA
Maximum Working Current	20 mA
Spot Diameter	4 mm

Fig. 3(b) plots the current, output power and applied voltage behavior. When the applied voltage is less than the threshold voltage, a small amount of current flows through the laser tube, and the output power is zero. At the threshold applied voltage, the current reaches the value required to produce electric discharge through the gas, and the lasing action starts in the cavity. Beyond the threshold voltage, the laser system's current and output power increases with applied voltage. The graph shows that the threshold voltage of the laser system is 9kV, and output power increases with the applied voltage. The maximum

Preprints (www.preprints.org) | NOT PEER-REVIEWED | Posted: 19 July 2022 doi:10.20944/preprints202207.0288.v1

output power of the laser system is 40 watts at the current of 10mA, as shown in Fig 3(b) [19]. The output power increases linearly with the applied voltage. The increase in applied voltage increases the discharge through the gas, resulting from which the excited state of CO_2 molecules gets heavily populated. In this process, a large number of photons are generated in the cavity, and the power of the output beam increases [20, 21].

6. PENETRATION RATE OF OUTPUT BEAM THROUGH DIFFERENT MATERIALS

The carbon dioxide laser is frequently used for cutting because of its high power. The laser beam's penetration depth at different output powers through the rock of pink salt (NaCl), acrylic sheet, and wood are analyzed.

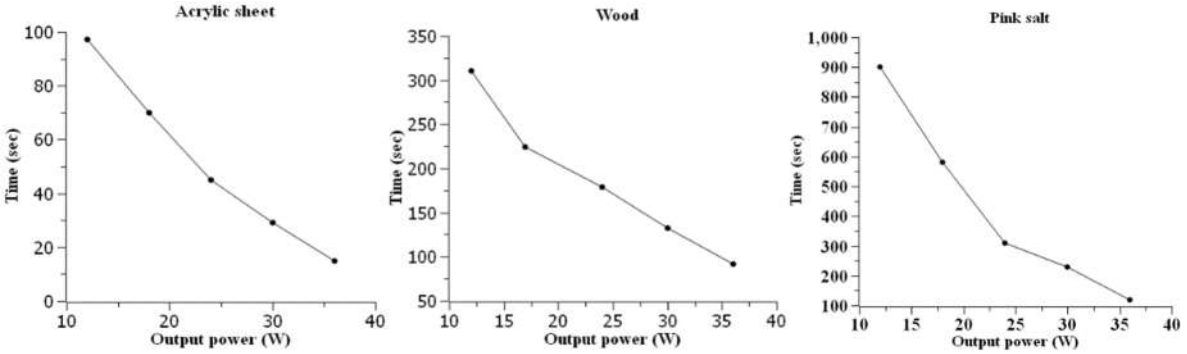

(a) **(b)** **(c)**

Fig. 4: Penetration time along output power for **(a)** Acrylic sheet (thickness=30mm) **(b)** Wood (thickness=12mm) **(c)** Rock of pink salt (thickness=5mm)

The above graph [Fig 4] shows that the beam will take less time to penetrate any material when the output beam power increases [22].

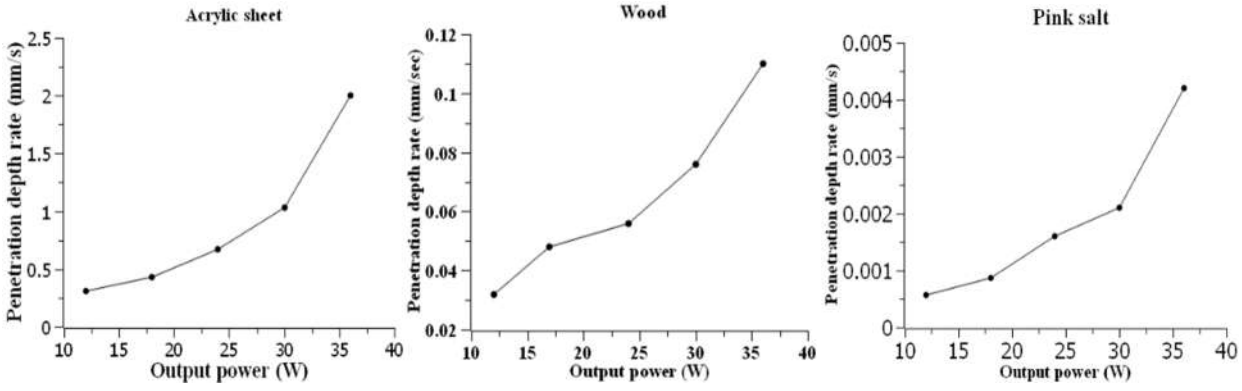

(a) **(b)** **(c)**

Fig. 5: Beam penetration rate along with output power **(a)** acrylic sheet **(b)** wood **(c)** rock of pink salt

The above graph [Fig 5] shows that the penetration rate through the salt, acrylic sheet, and wood increases with the output power increase. The penetration rate of the beam through salt and wood is less than that of the acrylic sheet. Most of the laser energy is utilized in burning wood; that's why the wood's penetration

Preprints (www.preprints.org) | NOT PEER-REVIEWED | Posted: 19 July 2022 doi:10.20944/preprints202207.0288.v1

rate is less than the acrylic sheet. The salt rock penetration rate is less because it has a very high melting point, and the beam takes more time to penetrate through the salt rock [23, 24].

7. CONCLUSION

Design, construction, and characterization of a very low-cost sealed tube medium power (40W) CO_2 laser system is presented, consisting of a prototype chiller and Flyback-based high voltage power supply. A high-tension pump source is designed to generate the required high voltage in the kilovolts(kV) range in the cavity, using the flyback transformer along with its flyback driver circuit. The output spark of the high voltage power supply is variable from 8kV to 30kV. A prototype cooling system is designed and constructed using a thermoelectric cooler (TEC) to maintain the laser cavity temperature. The cooling system can cool down the water up to 80C with a cooling rate of 0.7^0C/min, which is enough to compensate for the heat generated by the tube and make it stable for an extended period of its operation. The performance and efficiency of the cooling system at the different laser output power are studied, which shows that the chiller is stable and maintains the cavity temperature during the laser's long-time operation. The comparison of power, current and applied voltage indicate that the current flowing through the tube increases with an increase in the applied voltage so that laser output power increases. The spectrum of the CO_2 laser output is simulated using ZEMAX. The laser beam's penetration rate through the rock of pink salt, wood, and acrylic sheet at different output power is investigated, which shows that increasing the output power increases the penetration rate through the material.

DATA AVAILABILITY

The data that supports the findings of this study are available within the article [and its supplementary material].

CONFLICT OF INTEREST

On behalf of all authors, the corresponding author states that there is no conflict of interest.

REFERENCES

[1] Patel, C. K. N. "*Continuous-wave laser action on vibrational-rotational transitions of CO_2*", Physical review, Vol. 136(5A), pp. A1187, (1964).

[2] Patel, C.K.N. "*Selective Excitation Through Vibrational Energy Transfer and Optical Maser Action in N_2-CO_2*", Physical Review Letters, Vol. 13(21), pp. 617, (1964).

[3] Hanst, P.L. and Morreal, J.A. "*A Wavelength-Selective, Repetitively Pulsed CO_2 Laser*", Applied optics, Vol. 8(1), pp. 109-115, (1969).

[4] Thiebeaux, C., Delahaigue, A., Courtois, D. and Jouve, P. "*Design of a low-pressure CW carbon dioxide laser*", Infrared Physics, Vol. 21(1), pp. 41-44, (1981).

[5] Bilida, W. D., Strohschein, J. D., & Seguin, H. J. "*High-power 24-channel radial array slab rf-excited carbon dioxide laser*", In Gas and Chemical Lasers and Applications II, Vol. 2987, pp. 13-21, International Society for Optics and Photonics (1997).

[6] Nath, A. K., et al. "*High-power transverse flow CW CO_2 laser for material processing applications*", Optics & Laser Technology, Vol. 37(4), pp. 329-335, (2005).

[7] https://www.zemax.com/

[8] Naeem, M.; Fatima, N.-u.-a.; Hussain, M.; Imran, T.; Bhatti, A.S. "*Design Simulation of Czerny–Turner Configuration-Based Raman Spectrometer Using Physical Optics Propagation Algorithm*", Optics, Vol. 3, pp. 1–7, (2022). https://doi.org/10.3390/opt3010001

[9] Muddasir Naeem and Tayyab Imran. "*Design and Simulation of Mach-Zehnder Interferometer by Using ZEMAX Optic Studio*", Acta Scientific Applied Physics, Vol. 2(3), (2022).

[10] https://www.ni.com

[11] https://www.multisim.com

[12] Floyd, Thomas L. "*Electronic devices: conventional current version*", Pearson, (2012).

[13] Bondarev, A. V., Fedorov, S. V., & Muravyova, E. A. "*Control systems with pulse width modulation in matrix converters*", In *IOP Conference Series: Materials Science and Engineering*, Vol. 327(5), pp. 052008, (2018).

[14] Hussain, M., & Imran, T. "*Design and construction of prototype transversely excited atmospheric (TEA) nitrogen laser energized by a high voltage electrical discharge*", Journal of King Saud University-Science, Vol. 27(3), pp. 233-238, (2015).

[15] Naeem, M., Imran, T., Munawar, R., & Bhatti, A. S. "*Development of Low-Cost Prototype N2 Laser System and Laser-Induced Fluorescence of Pyranine*", Journal of Electrical and Electronic Engineering, Vol. 10(2), pp. 47-56, (2022).

[16] Hussain, M., & Imran, T. "*Experimental investigations of an efficient electric pump source for Blumlein-based TEA nitrogen laser*", International Journal of Scientific & Engineering Research, Vol. 8, pp. 1214-1219, (2017).

[17] Hussain, Mukhtar. "*Design and Fabrication of Prototype Transversely Excited Atmospheric (TEA) Nitrogen Laser*", Diss. COMSATS Institute of Information Technology Lahore-Pakistan, (2012).

[18] Liu, Yuming, et al. "*Design and Manufacture of a Pulse Driving Circuit for Semiconductor Laser*", Advancements in Mechatronics and Intelligent Robotics. Springer, Singapore, pp.441-447, (2021).

[19] Botero, G., et al. "*Design and performance of a sealed CO_2 laser for industrial applications*", Journal of Physics-Conference Series. Vol. 274(1), pp. 012058, (2011).

[20] Khan, N., et al. "*A Model of a Repetitively Pulsed Sealed-off CO 2 Laser*", Lasers in Engineering, Vol. 40 Issue 4-6, pp.277-296, (2018).

[21] Aram, M., Soltanmoradi, F., & Behjat, A. "*Investigation on parallel spark array pre-ionization TEA CO2 laser*", In Atomic and Molecular Pulsed Lasers V, Vol. 5483, pp. 43-50, International Society for Optics and Photonics, (2004).

[22] Auwal, S. T., et al. "*A review on laser beam welding of copper alloys*", The International Journal of Advanced Manufacturing Technology, Vol. 96(1), pp.475-490, (2018).

[23] Madić, M., Radovanović, M., Nedić, B., & Gostimirović, M. "*CO2 laser cutting cost estimation: mathematical model and application*", International Journal of Laser Science: Fundamental Theory and Analytical Methods, Vol. 1(2), pp. 169-183, (2018).

[24] Mushtaq, Ray Tahir, et al. "*State-of-the-art and trends in CO2 laser cutting of polymeric materials—a review*", Materials, Vol. 13(17), pp.3839, (2020).